中国光学（中英文） Chinese Optics 核心期刊

全圆锥入射下基于一维共振波导光栅的入射角调谐滤波器

樊丽娜 沙金巧 曹召良

Incident angle-tuned filter based on 1D resonant waveguide grating in full conical mounting

FAN Li-na, SHA Jin-qiao, CAO Zhao-liang

引用本文:
樊丽娜, 沙金巧, 曹召良. 全圆锥入射下基于一维共振波导光栅的入射角调谐滤波器[J]. 中国光学, 2024, 17(2): 493-500. doi: 10.37188/CO.EN-2023-0030
FAN Li-na, SHA Jin-qiao, CAO Zhao-liang. Incident angle-tuned filter based on 1D resonant waveguide grating in full conical mounting[J]. *Chinese Optics*, 2024, 17(2): 493-500. doi: 10.37188/CO.EN-2023-0030

在线阅读 View online: https://doi.org/10.37188/CO.EN-2023-0030

文章编号 2097-1842(2024)02-0493-08

Incident angle-tuned filter based on 1D resonant waveguide grating in full conical mounting

FAN Li-na*, SHA Jin-qiao, CAO Zhao-liang
(*School of Physical Science and Technology*, *Suzhou University of Science and Technology*, *Suzhou* 215009, *China*)
* *Corresponding author*, *E-mail*: *lnfan@mail.usts.edu.cn*

Abstract: This paper proposes and demonstrates a tunable filter using full conical mounting. The designed 1D resonant waveguide grating presents a tunable single reflection peak. The peak reflectance can theoretically reach 100%. The resonant wavelength can be tuned from 642.5 nm to 484.6 nm by changing the incident angle. The resonance between the 1st-order diffracted wave and fundamental transverse electric (TE) guided mode generates the reflection peak. This feature was achieved by optimizing the grating thickness to support the TE guided mode and suppress the transverse magnetic (TM) guided mode. The same concept can be applied to tunable filters with high dynamic range by increasing the thickness and period of grating in equal proportion.

Key words: tunable filters; resonant waveguide gratings; incident angle; full conical mounting

全圆锥入射下基于一维共振波导光栅的入射角调谐滤波器

樊丽娜*, 沙金巧, 曹召良
(苏州科技大学 物理科学与技术学院, 江苏 苏州 215009)

摘要: 本文提出并展示了一种全圆锥入射下基于一维共振波导光栅的入射角调谐滤波器。通过优化光栅层厚度, 使其能够在支持 TE 导模的同时抑制 TM 导模。本文设计的滤波器呈现出可调谐的单一反射峰, 峰值反射率理论上可达 100%。当入射角改变时, 共振波长可以由 642.5 nm 调节至 484.6 nm。该反射峰是由一级衍射波与 TE 导模(基模)之间的共振效应所产生的。同样地, 通过按比例增加光栅层的厚度和周期可实现应用于更高动态范围的可调谐滤波器。

关 键 词: 可调谐滤波器; 共振波导光栅; 入射角; 全圆锥装配
中图分类号: O436.1;TN25 **文献标志码:** A **doi:** 10.37188/CO.EN-2023-0030

收稿日期: 2023-11-19; **修订日期:** 2023-12-05
基金项目: "十四五"江苏省重点学科资助(No. 2021135); 吉林省科技厅重点研发项目(No. 20220203033SF)
Supported by Jiangsu Key Disciplines of the Fourteenth Five-Year Plan (No. 2021135); Key Research and Development Project of the Department of Science and Technology of Jilin Province (No. 20220203033SF)

1 Introduction

Resonant waveguide gratings (RWGs) can achieve narrowband reflection or transmission resonant spectrum by utilizing periodic grating to couple the incoming light into a thin waveguide[1-2]. The filtered spectrum, including wavelength, linewidth, sideband, and intensity, can be tailored. RWGs have been extensively investigated in diverse applications[3-4] due to their highly adjustable performance. High-efficiency tunable narrowband filters[5-6] are desirable components in various biomedical and industrial applications since they allow a device to be adapted to different wavelengths. Some tunable narrowband filters based on one-dimensional (1D) and two-dimensional (2D) RWGs have been proposed. The 2D structures have a certain complexity in modeling geometries and fabrication techniques[7-8]. The 1D structures show the potential for easy fabrication using well-established processes[9-10].

In this paper, the focus is specifically on tuning the resonant wavelength of 1D RWGs. The basic approach is mechanically changing the grating parameters[11-12], such as the grating period[11], to realize wavelength tuning. The active approach is to implement thermo-optic[13] or electro-optic modulation[14] to induce a change in the refractive index. Dynamically adjusting the incident angle[15-16] and azimuth angle[17-18] of the incoming light is another promising approach to achieving wavelength tuning for a given device. The light paths of incident angle modulation in classical mounting is simple. However, the oblique incidence gives rise to the splitting of a single resonant peak[19]. Azimuth angle modulation can achieve polarization-insensitive filters[20]. However, the approach requires adjusting the incident and azimuth angles on two dimensions.

1D RWGs are intrinsically angle-sensitive devices[21-22]. The incoming light may lie in two specific incident planes, namely, classical mounting (with the incident plane perpendicular to the grooves of the grating) and full conical mounting (with the incident plane parallel to the grooves of the grating)[23-25]. In this paper, the incident light lies in the full conical incident plane. The designed 1D RWG exhibits effective wavelength tuning with the incident angle's variation under this incident condition. The proposed method can avoid the deficiencies of incident angle modulation in classical mounting and azimuth angle modulation in conical mounting.

2 Tuning method and results

The proposed filter is based on a conventional single-layer 1D RWG structure, as illustrated in Figure 1. The substrate and the environment medium surround the grating layer. The subwavelength grating layer has a higher effective refractive index than its surrounding media, so it also acts as a waveguide layer in the designed structure. The rectangular grating parameters are as follows: ridge refractive index of the grating n_{H}, groove refractive index of the grating n_{L}, grating period Λ, fill factor f, grating thickness d, refractive index of the substrate n_{s}, and refractive index of the environment medium n_{c}. The thickness of the substrate and environment medium was assumed to be greater than the grating thickness. Rigorous coupled wave analysis (RCWA)[26] was used to calculate the spectral responses for the proposed device in this paper. In accordance with the guided mode resonance (GMR) effect, the position of the resonant wavelength can be modulated by altering the above structural parameters[27-28]. This paper aims to realize wavelength tuning through the adjustment of incident conditions such that the plane light wave irradiates the designed 1D RWG at a variable angle in the specific full conical mounting ($\varphi = 90°$). Through optimizing the structural parameters, the coupling between diffracted waves and guided modes was realized at a large range of incident angles.

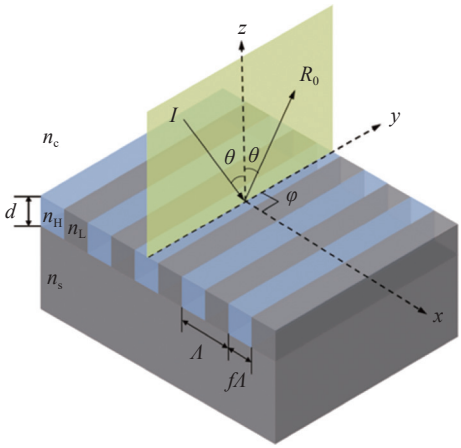

Fig. 1　Schematic diagram of 1D RWG in full conical mounting. The structural parameters are n_H = 1.8, n_L = 1.63, n_s = 1.46, n_c = 1.0, d = 102 nm, f = 0.5, and Λ = 440 nm

In the case of non-full conical mounting, since the asymmetry of the ±ith-order diffracted waves, resonance may occur between the evanescent ±ith-order diffracted waves and the guided modes with different polarization states. On the contrary, full conical mounting reduces the probability of resonance by half because the guided modes excited by the ±ith-order diffracted waves are degenerated at oblique incidence in full conical mounting[23]. However, the guided modes may have two polarization states (TE and TM) in full conical mounting[25]. Here, the grating thickness was engineered to support the certain guided mode (fundamental TE), which was excited by the symmetrical ±1st-order diffracted waves. After optimizing, the single resonant peak could be ensured over a large range of incident angles in full conical mounting.

The incident angle of TM-polarized incoming light was changed to obtain different resonant wavelengths from the same 1D RWG by a RCWA algorithm. As shown in Figure 2 (color online), the center wavelengths of resonant peaks drifted to short wavelengths when the incident angle increased. As the incident angle increased from 0° to 80°, the resonant wavelength (λ_R) tuning ranged from 642.5 nm to 484.6 nm. The reflectance of resonant peaks remained almost constant at 100% as the incident angle changed. This feature resulted from maintaining the high coupling efficiency between the diffracted wave and the guided mode when the incident angle changed from 0° to 80°. The sidebands of these resonant peaks first decreased and then increased with the increase in incident angle. The mean sideband reflectance was less than 20% in incident angle modulation, indicating that the sidebands can be effectively suppressed from 0° to 80°. This feature reveals that TM incidence can handle low sideband reflectance. The sideband of the resonant peak was the lowest when the incident angle was 60°, which can be explained by the Brewster effect. According to the effective medium theory, the effective refractive index of the grating for the TM-polarized wave was $n_{eff} = 1/\sqrt{(1-f)/n_L^2 + f/n_H^2} = 1.709$, and the corresponding Brewster angle was 59.66°, which is around 60°. Furthermore, the reflection peak's linewidth increased with the increase in the incident angle. When the incident angles were 0°, 20°, 40°, 60°, and 80°, the linewidths were 0.23, 0.36, 0.64, 0.90, and 1.82 nm, respectively.

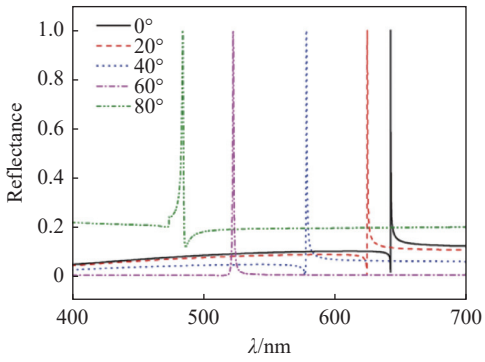

Fig. 2　Calculated reflection spectra with the incident angle variation when the TM-polarized wave irradiates 1D RWG in full conical mounting

For clarity, the normalized amplitude of the internal electric field (E_y) profile at various resonant wavelengths is plotted along with the corresponding incident angles. Figure 3 (color online) illustrates the E_y profile in a cross-sectional xz plane over one grating period. The bound-guided mode was the fundamental TE mode in the longitudinal direction (z direction). The leaky guided mode along

the structure formed lateral standing wave patterns (x direction). They exhibited strong field localization in the grating layer, that is, the waveguide layer in the designed structure. This electric field distribution confirmed the mechanism of resonant wavelength tuning. The change in incident angle caused the occurrence of resonance at different wavelengths. The standing wave patterns showed local electric field strength. As shown in Figure 3, the strongest field region gradually moved from the substrate to the grating layer with the increase in incident angle. This happened because the effective refractive index of the fundamental TE guided mode at the short resonant wavelength region was larger than that at the long resonant wavelength region. The bound ability of the waveguide layer to the guided mode was significantly enhanced because the refractive index of the waveguide layer became higher compared with the refractive index of the surrounding media.

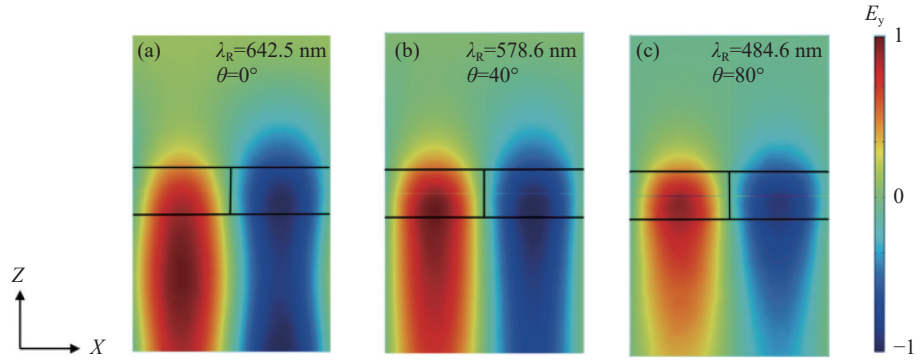

Fig. 3 Internal electric field (E_y) profile for (a) λ_R = 642.5 nm (θ = 0°); (b) λ_R = 578.6 nm (θ = 40°); (c) λ_R = 484.6 nm (θ = 80°)

3 Analysis and discussion

In accordance with the basic principle of the GMR effect, the phase-matching condition in full conical mounting is

$$\beta_m = k_0 \sqrt{n_c^2 \sin^2\theta + i^2 \frac{\lambda^2}{\Lambda^2}} \quad , \qquad (1)$$

where β_m is the propagation constant of the m-th guided mode, $k_0 = 2\pi/\lambda$, λ is the wavelength of the incident light, and i is the diffraction order. The eigenvalue equations of the waveguide are expressed as

$$\tan(k_m d) = \frac{k_m(\gamma_m + \delta_m)}{k_m^2 - \gamma_m \delta_m}, \text{TE} \quad , \qquad (2)$$

$$\tan(k_m d) = \frac{n_{eff}^2 k_m (n_s^2 \gamma_m + n_c^2 \delta_m)}{n_s^2 n_c^2 k_m^2 - n_{eff}^4 \gamma_m \delta_m}, \text{TM} \quad , \qquad (3)$$

where $\gamma_m = (\beta_m^2 - k_0^2 n_s^2)^{1/2}$, $k_m = (k_0^2 n_{eff}^2 - \beta_m^2)^{1/2}$ and $\delta_m = (\beta_m^2 - k_0^2 n_c^2)^{1/2}$ are the wave numbers along the z-axis direction in the cover layer, grating layer, and substrate, respectively.

The resonant wavelength can be approximately calculated by using the phase matching condition [Eq. (1)] and eigenvalue equation of the waveguide [Eq. (2) & Eq. (3)]. When the conditions are satisfied, a certain order-guided mode may be excited by the certain order-diffracted wave. Figure 4 (color online) indicates the calculated resonant wavelength positions for various incident angles from 0° to 80°. The curves plotted in accordance with the eigenvalue equation represent the relationship between the resonant wavelength and grating thickness, where the 1st-order diffracted wave resonated with the fundamental TE guided mode (denoted as $TE_{1,0}$) under the irradiation of various incident angles. The curves did not split under oblique incidence because of the symmetry of ±1st-order diffracted waves in full conical mounting. The straight line of d/Λ = 0.232 was calculated in accordance with the structural parameters. The intersections of the curves and the straight line show the resonant positions for the proposed structure with

the changing incident angle. As shown in Figure 4, all the curves moved down as the incident angle increased. When the incident angle varied by several given values, a point of intersection was always found between the curve and the straight line. The resonant positions corresponding to these intersections show excellent agreement with the resonant wavelength in Figure 2. The resonance behavior was sustained when the incident angle varied from 0° to 80°. Figure 4 reveals that the 1D RWG can perform dynamic filtering by changing the incident angle in full conical mounting. The eigenvalue equation is a function of the propagation constant and depends on the incident angle. With the occurrence of resonance, the resonant wavelength changed in correspondence with the incident angle variation.

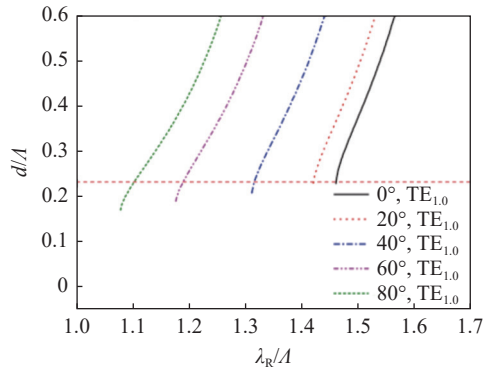

Fig. 4　Calculated resonant positions based on the eigenvalue equation of fundamental TE guided mode at different incident angles

The grating thickness was engineered to exhibit only single-mode propagation in the waveguide so that the structure presented a single peak during the modulation of the incident angle. This process was performed to ensure nonchaotic tuning. RWGs may support various guided modes with TE and TM polarizations in full conical mounting. Similar to Figure 4, we calculated the resonant positions on the basis of the eigenvalue equation of fundamental TE and TM guided modes through sampling at incident angles of 0°, 40°, and 80°. As Figure 5 (color online) shows, these curves moved down as the incident angle decreased regardless of the coupling between the 1st-order diffracted wave and the fundamental TE guided mode or the fundamental TM guided mode (denoted as $TE_{1,0}$ and $TM_{1,0}$, respectively). The optimization of grating thickness proved crucial in 1D RWG. When d/Λ was less than 0.228, the grating thickness did not support the generation of resonance. In that case, there was no initial peak at normal incidence. And the peak only appeared when the incident angle increased to a certain value. When d/Λ was greater than 0.266, the 1st-order diffracted wave resonated simultaneously with the fundamental TE and TM guided modes, resulting in the formation of two peaks at the incident angle of 80°. The value of d/Λ was within a certain interval of 0.228 to 0.266, which is marked by the red dotted box in Figure 5. The single peak always comes from the coupling of the 1st-order diffracted wave and the fundamental TE guided mode. This supports the idea that the single resonant wavelength can be tuned at angles ranging from 0° to 80°.

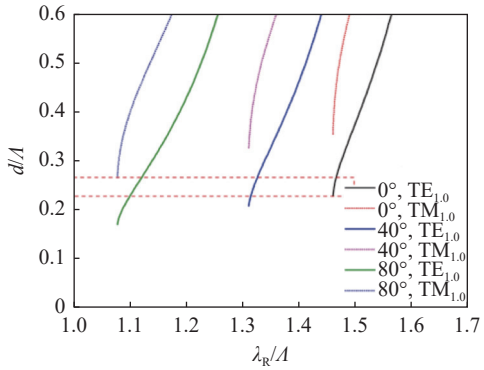

Fig. 5　Calculated resonant positions based on the eigenvalue equation of fundamental TE and TM guided modes at different incident angles

The proposed structure also performs a filtering function when irradiated by TE-polarized incoming light; however, it is not optimal as an angle-tuned filter in full conical mounting because it is difficult to suppress the sideband reflectance when the incident angle is adjusted. Here, the grating layer is equivalent to a thin film layer. The sideband reflectance of RWG is essentially the reflectance of a multilayer stack outside the resonant peak. This means that outside the resonant peak, the RWG's reflectance can be understood in terms of the multilayer stack properties without the influence of the res-

onant enhancement. We calculated the reflection spectra of equivalent multilayer stacks with TE- and TM-polarized incoming light at different incident angles. For TE-polarized incidence, as Figure 6(a) (color online) shows, the reflectance increased sharply and monotonously as the incident angle increased from 0° to 80°. At the incident angle of 60°, the mean reflectance was approximately 30%. High sideband reflectance affected the recognition of the reflected filtering signal. For TM-polarized incidence, as Figure 6(b) (color online) shows, the reflectance decreased as the incident angle increased when the incident angle was lower than the Brewster angle. The reflectance was almost zero near the Brewster angle. Subsequently, the reflectance increased as the incident angle increased. These results are consistent with the sidebands of resonant peaks shown in Figure 2. For the same incident angle, the reflectance with TM-polarized incoming light was lower than that with TE-polarized incoming light. This results from the strong suppression of reflectance by the Brewster effect in the TM polarization state.

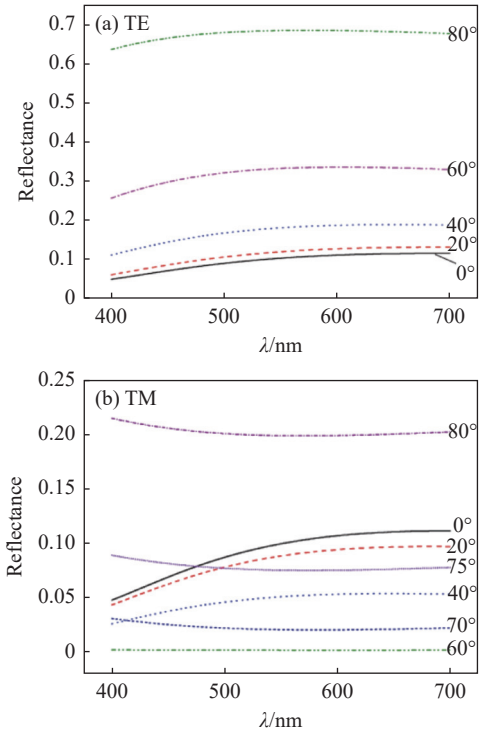

Fig. 6 Reflection spectra of equivalent multilayer stacks at different incident angles. (a) TE-polarized incidence; (b) TM-polarized incidence

Figure 7 shows the resonant wavelengths for various incident angles in full conical mounting to explore the tuning performance. The data was fitted by a cubic polynomial function. Here, the tuning rate is defined as the shift of resonant wavelength over the change in the incident angle ($\Delta\lambda_R/\Delta\theta$) in nanometers per degree. The tuning rate was low in the large angle areas of 75°−80° and small angle areas of 0°−10°. The proposed 1D RWG can perform wavelength modulation when the incident angle varies from 0° to 80°. The wavelength tuning range is approximately 157 nm with a variable tuning rate.

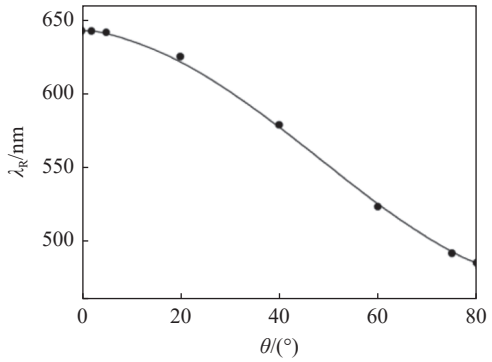

Fig. 7 Resonant wavelength as a function of the incident angle

The tuning rate and range can be extended by altering the value of d and Λ in the proposed structure. The thickness and period of grating increase simultaneously in equal proportion. Here, the proportionality factor is defined as k. The dispersion effect of materials is ignored. In this way, the resonant spectra are similar in form to the spectra before k value amplification, except for the peak's resonant wavelength position and linewidth. This resonant spectrum has a wavelength of $\lambda_R' = k \times \lambda_R$ with the linewidth of $FWHM' = k \times FWHM$ at the equivalent angle incidence. Figure 8 (color online) shows the result of the resonant wavelength as a function of the k value and the incident angle. With an equivalent incident angle, the resonant wavelength increases linearly with the k value in a direct proportion. In addition, the tuning rate and range increase in proportion to the increase in k value. For the proposed structure with k = 2.5, the other parameters

are consistent with Figure 1. The tuning range is from 1 606.2 nm to 1 211.5 nm when the incident angle varies from 0° to 80°. This result implies that a broader spectral range may be reached by changing the thickness and period of grating without considering the dispersion.

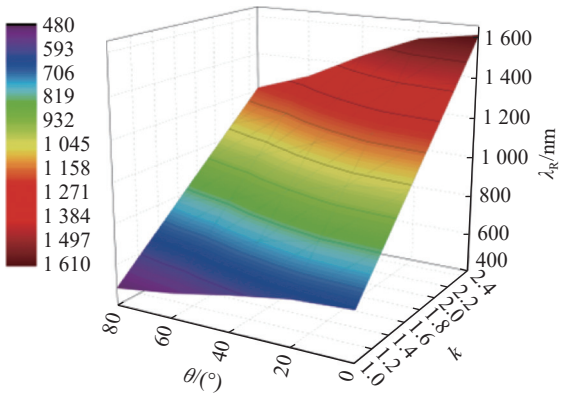

Fig. 8　Resonant wavelength as a function of the k value and the incident angle

4　Conclusion

In summary, this paper describes a numerical study of the tunable filtering characteristics of 1D RWG in full conical mounting. A tunable reflection filter with high performance was proposed and demonstrated by incident angle modulation. The full conical mounting provided the degenerated guided modes excited by the ±1st-order diffracted waves at oblique incidence. Under the condition of this certain incident plane, the grating thickness was optimized to obtain a single resonant peak. It was also demonstrated that TM incidence exhibits better suppression of sideband reflectance than TE incidence for angle-tuned filters in full conical mounting. These factors, including incident conditions and grating thickness, improved the filter's performance. Furthermore, the spectral dynamic range of the proposed method can be extended by reconfiguring the thickness and period of grating. The numerical results demonstrate the achievement of tunability over a wavelength range of roughly 1 210 nm to 1 600 nm. The proposed tunable filter has potential applications in biomedical optical imaging.

References:

[1] FENG S Q, LIU T T, CHEN W Y, *et al*.. Enhanced sum-frequency generation from etchless lithium niobate empowered by dual quasi-bound states in the continuum[J]. *Science China Physics, Mechanics & Astronomy*, 2023, 66(12): 124214.

[2] WU F, WU J J, GUO ZH W, *et al*.. Giant enhancement of the Goos-Hänchen shift assisted by quasibound states in the continuum[J]. *Physical Review Applied*, 2019, 12(1): 014028.

[3] QIAN L Y, WANG K N, ZHU W, *et al*.. Enhanced sensing ability in a single-layer guided-mode resonant optical biosensor with deep grating[J]. *Optics Communications*, 2019, 452: 273-280.

[4] HSU H Y, LAN Y H, HUANG CH SH. A gradient grating period guided-mode resonance spectrometer[J]. *IEEE Photonics Journal*, 2018, 10(1): 4500109.

[5] FEHREMBACH A L, SHARSHAVINA K, LEMARCHAND F, *et al*.. 2 × 1D crossed strongly modulated gratings for polarization independent tunable narrowband transmission filters[J]. *Journal of the Optical Society of America A*, 2017, 34(2): 234-240.

[6] QIAN L Y, ZHU W, WANG K N, *et al*.. Polarization-controlled reflectance tunable narrow-band filter with single channel based on sparse dielectric grating[J]. *Optics Communications*, 2019, 443: 123-128.

[7] KUO W K, HSU C J. Two-dimensional grating guided-mode resonance tunable filter[J]. *Optics Express*, 2017, 25(24): 29642-29649.

[8] FERRARO A, TANGA A A, ZOGRAFOPOULOS D C, *et al*.. Guided mode resonance flat-top bandpass filter for terahertz telecom applications[J]. *Optics Letters*, 2019, 44(17): 4239-4242.

[9] SAKAT E, VINCENT G, GHENUCHE P, *et al*.. Free-standing guided-mode resonance band-pass filters: from 1D to 2D structures[J]. *Optics Express*, 2012, 20(12): 13082-13090.

[10] SALEEM M R, ZHENG D D, BAI B F, *et al*.. Replicable one-dimensional non-polarizing guided mode resonance gratings under normal incidence[J]. *Optics Express*, 2012, 20(15): 16974-16980.

[11] FANG CH L, DAI B, LI ZH, *et al*.. Tunable guided-mode resonance filter with a gradient grating period fabricated by casting a stretched PDMS grating wedge[J]. *Optics Letters*, 2016, 41(22): 5302-5305.

[12] FENG SH F, ZHANG X P, SONG J Y, *et al*.. Theoretical analysis on the tuning dynamics of the waveguide-grating structures[J]. *Optics Express*, 2009, 17(2): 426-436.

[13] CHAUDHURI R R, ENEMUO A N, SONG Y, *et al*.. Polymer based resonant waveguide grating photonic filter with on-chip thermal tuning[J]. *Optics Communications*, 2018, 418: 1-9.

[14] WANG C T, HOU H H, CHANG P C, *et al*.. Full-color reflectance-tunable filter based on liquid crystal cladded guided-mode resonant grating[J]. *Optics Express*, 2016, 24(20): 22892-22898.

[15] UDDIN M J, MAGNUSSON R. Efficient guided-mode-resonant tunable color filters[J]. *IEEE Photonics Technology Letters*, 2012, 24(17): 1552-1554.

[16] COVES Á, GIMENO B, ANDRÉS M V. Oblique incidence and polarization effects in coupled gratings[J]. *Optics Express*, 2012, 20(23): 25454-25460.

[17] YUKINO R, SAHOO P K, SHARMA J, *et al*.. Wide wavelength range tunable one-dimensional silicon nitride nano-grating guided mode resonance filter based on azimuthal rotation[J]. *AIP Advances*, 2017, 7(1): 015313.

[18] REN ZH B, SUN Y H, HU J SH, *et al*.. Nonpolarizing guided-mode resonance filter with high tolerance of conical angle[J]. *Journal of Optics*, 2018, 20(8): 085601.

[19] WANG D Y, WANG Q K, WU M T. Spectral characteristics of a guided mode resonant filter with planes of incidence[J]. *Applied Optics*, 2018, 57(27): 7793-7797.

[20] WANG W, CAI W, SHI ZH, *et al*.. Polarization-insensitive one-dimensional guided-mode resonance filter operating at conical mounting[J]. *Optics Letters*, 2018, 43(21): 5226-5229.

[21] KODALI A K, SCHULMERICH M, IP J, *et al*.. Narrowband midinfrared reflectance filters using guided mode resonance[J]. *Analytical Chemistry*, 2010, 82(13): 5697-5706.

[22] LI Y Y, HU CH, WU Y CH, *et al*.. Numerical investigation of one-dimensional nonpolarizing guided-mode resonance gratings with conformal dielectric films[J]. *Optics Express*, 2013, 21(1): 345-357.

[23] FAN L N, JIA K H, MA J SH. Transmission filter controlled by incident conditions in single-layer waveguide grating structures[J]. *Applied Optics*, 2019, 58(31): 8371-8375.

[24] WANG D Y, WANG Q K, LIU D M. Polarization-insensitive filter for incidence between classic and full conical mountings[J]. *IEEE Photonics Technology Letters*, 2018, 30(5): 495-498.

[25] LACOUR D, GRANET G, PLUMEY J P, *et al*.. Polarization independence of a one-dimensional grating in conical mounting[J]. *Journal of the Optical Society of America A*, 2003, 20(8): 1546-1552.

[26] MOHARAM M G, GAYLORD T K. Diffraction analysis of dielectric surface-relief gratings[J]. *Journal of the Optical Society of America*, 1982, 72(10): 1385-1392.

[27] MAGNUSSON R, WANG S S. New principle for optical filters[J]. *Applied Physics Letters*, 1992, 61(9): 1022-1024.

[28] WANG S S, MAGNUSSON R. Theory and applications of guided-mode resonance filters[J]. *Applied Optics*, 1993, 32(14): 2606-2613.

Author Biographics：

Fan Li-na (1980—), female, Yuci city, Shanxi province, Ph.D., received her Ph.D. from the University of Shanghai for Science and Technology in 2020 and is mainly engaged in research on micro-nano optical devices. E-mail: lnfan@mail.usts.edu.cn